LIMNOLOGY and OCEANOGRAPHY

ASLO

Limnol. Oceanogr. 69, 2024, 1218–1232

doi: 10.1002/lno.12564

Ubiquitous but unique: Water depth and oceanographic attributes shape methane seep communities

Sarah Seabrook,[1*] **Marta E. Torres**,[2] **Tamara Baumberger**,[3] **David Butterfield**,[4,5] **Kevin Roe**,[4] **Milo Cummings**,[6] **Rebecca Crawford**,[2,a] **Andrew R. Thurber**[2,6]

[1]National Institute of Water and Atmospheric Research, Wellington, New Zealand
[2]College of Earth, Ocean and Atmospheric Sciences, Oregon State University, Corvallis, Oregon, USA
[3]Oregon State University and NOAA Pacific Marine Environmental Laboratory, Hatfield Marine Science Center, Newport, Oregon, USA
[4]University of Washington, Cooperative Institute for Climate and Ocean Ecosystem Studies, Seattle, Washington, USA
[5]NOAA Pacific Marine Environmental Laboratory, Cooperative Institute for Climate and Ocean Ecosystem Studies, Seattle, Washington, USA
[6]Department of Microbiology, College of Science, Oregon State University, Corvallis, Oregon, USA

Abstract

In the past decade, thousands of previously unknown methane seeps have been identified on continental margins around the world. As we have come to appreciate methane seep habitats to be abundant components of marine ecosystems, we have also realized they are highly dynamic in nature. With a focus on discrete depth ranges across the Cascadia Margin, we work to further unravel the drivers of seep-associated microbial community structure. We found highly heterogenous environments, with depth as a deterministic factor in community structure. This was associated with multiple variables that covaried with depth, including surface production, prevailing oxygen minimum zones (OMZs), and geologic and hydrographic context. Development of megafaunal seep communities appeared limited in shallow depth zones (~ 200 m). However, this effect did not extend to the structure or function of microbial communities. Siboglinid tubeworms were restricted to water depths > 1000 m, and we posit this deep distribution is driven by the prevailing OMZ limiting dispersal. Microbial community composition and distribution covaried most significantly with depth, but variables including oxygen concentration, habitat type, and organic matter, as well as iron and methane concentration, also explained the distribution of the microbial seep taxa. While members of the core seep microbiome were seen across sites, there was a high abundance of microbial taxa not previously considered within the seep microbiome as well. Our work highlights the multifaceted aspects that drive community composition beyond localized methane flux and depth, where environmental diversity adds to margin biodiversity in seep systems.

Methane seeps are dynamic marine ecosystems where chemical-rich fluids (e.g., methane, sulfide) support microbial processes that create habitat heterogeneity (Cordes et al. 2010) and food for the surrounding environment (Levin and Michener 2002; MacAvoy et al. 2002). Once considered to be oases that stood in stark contrast to an otherwise sparse deep sea, a much broader "sphere of influence" is now increasingly recognized for seeps (Levin et al. 2016). In addition, these environments have been shown to interact with, and be epicenters of, a diverse suite of ecosystem functions and services, ranging from commercial fisheries production to global climate modulation (Grupe et al. 2015; Seabrook et al. 2019; Turner et al. 2020).

Chemosynthetic microbial taxa at seep sites work as microbial ecosystem engineers, converting chemical energy into biomass that can be harvested as food by other organisms

*Correspondence: sarah.seabrook@niwa.co.nz

[a]Present address: University of Victoria, Victoria, Canada

Additional Supporting Information may be found in the online version of this article.

Author Contribution Statement: SS, ART, and MET conceived of the study framework and wrote the manuscript. SS, DB, KR, MC, RC, and ART contributed to sample analysis as well as data analysis. SS, TB, DB, KR, and RC participated in field work and sample collection. SS, MET, MC, and ART made or contributed to figures within the manuscript. All authors contributed to editing the manuscript.

(Niemann et al. 2013), creating substrate (Luff and Wallmann 2003), and mitigating the release of methane—a potent greenhouse gas—into the atmosphere (Sommer et al. 2006). The foundational engineering microbial taxa are a distinct community collectively known as the "global seep microbiome" (Ruff et al. 2015). ANerobic MEthane (ANME) oxidizing archaea are arguably the most highlighted seep microbial taxa and can work in consortia with bacterial partners (e.g., sulfate-reducing bacteria) to oxidize up to 90% of methane at marine methane seeps (Knittel and Boetius 2009). Aerobic methane-oxidizing (e.g., Methanococcalles) and sulfide-oxidizing (e.g., Camplyobacterales, Beggiatoales) bacteria are also considered important components of the seep microbiome. Within seep ecosystems, seep-endemic animals (e.g., siboglinid tubeworms, vesicomyid clams, mytilid mussels) derive nutrition from thiotrophic and methanotrophic microbial symbionts and microbial biomass from chemosynthetic primary production is transferred to non-seep-specific food webs (e.g., Levin and Michener 2002; Seabrook et al. 2019). Carbonate precipitation resulting from anaerobic methane oxidation leads to platforms and boulders that persist for hundred-to-thousand-year timescales (Kulm et al. 1986) and provide substrate for a diversity of species (e.g., cold-water corals and sponges), impacting marine biodiversity in a multitude of ways. The development of authigenic carbonate can also act to terminate or shift fluid flow at seepage sites.

The first methane seep was discovered almost 40 yr ago (Paull et al. 1984; Kulm et al. 1986), and since then, these habitats have increasingly become appreciated as ubiquitous centers of biogeochemical cycling on continental margins. High carbon input coupled with burial and/or subduction processes over geologic timescales has created large reservoirs of reduced carbon in the subsurface of continental margins (Claypool and Kaplan 1974). These carbon reservoirs can manifest as gas-filled reservoirs and/or gas hydrates, which may be identifiable in seismic surveys and have been correlated to free gas emissions imaged in water column hydroacoustic surveys (e.g., Greinert et al. 2010). With these methods, thousands of methane seeps have been found across active (e.g., Johnson et al. 2015; Watson et al. 2020; Merle et al. 2021) and passive (e.g., Skarke et al. 2014; Mau et al. 2017) margins. With the increased quantification of seep abundance, there has been a concomitant increase in our awareness of the high heterogeneity of seep habitats, across depth, latitude, biogeochemical, and productivity gradients (Levin et al. 2003; Seabrook et al. 2018). While bottom-up control of seep ecosystems by fluid flow is evident, the importance and magnitude of other environmental drivers in shaping the many varied seep systems of continental margins is less understood.

Across the many newly discovered seep habitats described to date, enigmatic patterns exist, such as latitudinal patterns in biodiversity within the seep microbiome (Seabrook et al. 2018) and the impact of seepage on defining microbial communities (Ruff et al. 2015). Here, we explore the drivers of seep structure at the micro-scale and broader habitat-scale along parallel depth transects on the Cascadia Margin. We ask (1) how seep structure varies across the margin environment and (2) how environmental variables (e.g., depth, oxygen concentration) correlate with the observed gradients in microbial distributions. Through this regional-scale analysis, we advance our understanding of the multifaceted drivers of seep dynamics.

Methods

Setting

Gas seepage across the Cascadia Margin, the continental margin offshore British Columbia to Northern California, is widespread (Johnson et al. 2015) and substantial (Riedel et al. 2018), with thousands of seeps identified (Merle et al. 2021) to date with dozens studied in more detail (e.g., Baumberger et al. 2018 and references within). The presence of gas reservoirs at depth and the prevalence of gas hydrate deposits has been well documented in seismic data as well as by scientific ocean drilling in this margin (e.g., Tréhu et al. 2004*b*). The Cascadia Margin is characterized by a persistent oxygen minimum zone (OMZ) between the depths of about 650–1100 m (Guilini et al. 2012), with the boundaries of the OMZ defined here as regions with oxygen concentrations below approximately 22 μmol L^{-1} (Gooday et al. 2010; see Supporting Information Fig. S6 for full water column profiles of oxygen concentration across the sites studied here). Prevailing oceanographic conditions create shifts in upwelling-supported primary production (e.g., Spitz et al. 2003). Episodic runoff inputs from both a major river system (i.e., the Columbia River) and small mountainous river systems influence fluxes of dissolved and particulate carbon (Goñi et al. 2013). Earthquakes, faulting, and volcanic activity, as well as bathymetric changes, are associated with the geodynamics of this active subduction zone (e.g., Goldfinger et al. 2003). Furthermore, seafloor processes along the Cascadia Margin provide ecosystem service value that benefits humans, including the fisheries market that depends on the productivity of the whole system. Notably, methane seeps are increasingly considered part of these human benefits, as evidenced by the inclusion of methane seeps as essential fish habitats in the region (Shester et al. 2021).

Study area

In this study, we focused on three regions along the Cascadia Margin in the Northeast Pacific Ocean: (1) Astoria Canyon (AC); (2) Heceta Banks (HB); (3) Coquille (CQ) (Fig. 1; Supporting Information Table S1). Within these three regions, we defined four distinct depth ranges between 150 and 1400 m, including shallow (100–200 m), mid (400–800), the minima of the OMZ (< 6 μmol L^{-1} and 750–800 m here), and deep sites (1000–1400 m). Of the sites explored within this study, we were able to retrieve sediment samples from all but the shallow Heceta Banks site, due to the benthos at the shallow Heceta Banks being unsuitable for coring. In this paper,

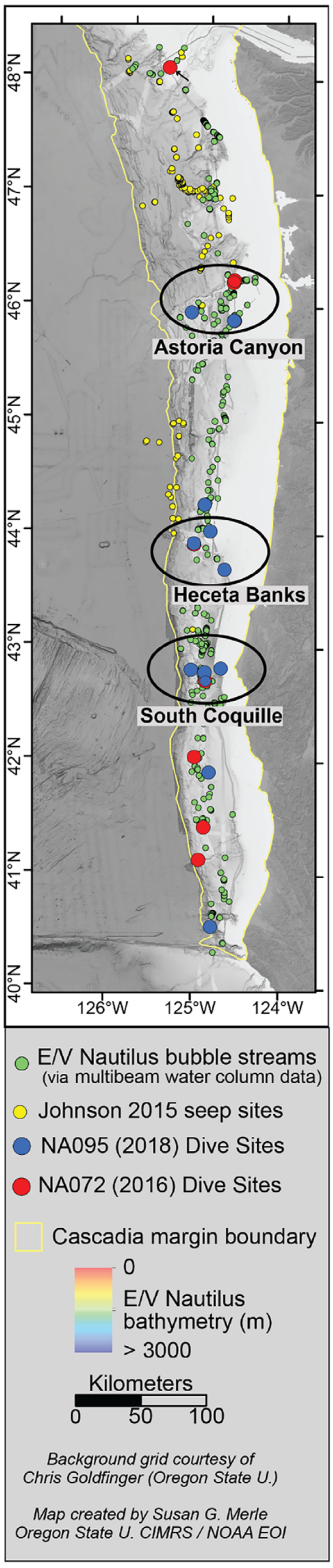

Fig. 1. Map of study sites included in this paper. Sites explored on both the NA072 (red dots) and NA095 (blue dots) cruise aboard the EV *Nautilus* with Ocean Exploration Trust are indicated. Green dots are bubble streams identified by EV *Nautilus* from 2016 to 2018, yellow dots indicate bubble streams published by Johnson et al. (2015).

these sites will be referred to by their name and mean depth (e.g., AC190; Supporting Information Table S1). The site descriptions provided, including seep megafauna and structure observed, are qualitative observations from the time spent exploring the seep sites with the ROV. The time spent at each site collecting these observations (on bottom time) is provided in Supporting Information Table S1.

Water column geochemical measurements

Sensors onboard the ROV *Hercules* were used to measure metrics in the water column above the seep sites. Oxygen concentration was measured by an oxygen optode (Aanderaa 3830), and the values provided are from approximately 0.5 m above the seafloor. Temperature, depth, and conductivity were measured with a Sea-Bird FastCAT 49. Data provided in Supporting Information Table S1 is averaged from all data collected while on the bottom at the seep sites and rounded to the nearest significant figure provided.

Sediment and geochemical sampling

Samples were collected during cruises NA095 and NA072 aboard the EV *Nautilus*. Push core samples (internal diameter 6.4 cm) were taken by the ROV *Hercules* from seep habitats at each of the sites (Fig. 1; Supporting Information Table S1). Samples were collected from the representative microbial mat, clam bed, and "background" sediment habitat zonation's within each site whenever possible. Background sediments were defined as areas a minimum of 100 m away from the last observed signatures of active seepage (e.g., microbial mats, bubbles, carbonates, reduced sediment, and seep fauna). Upon retrieval, cores were extruded and sectioned at 1 cm intervals, with the sides of the cores discarded to avoid smearing and frozen at −80°C. Select cores were sampled for porewater using Rhizon samplers before extrusion. Sediment porewaters were preserved and analyzed for various metrics, including methane, sulfide, and sulfate, as described in Supporting Information (also *see* Supporting Information Tables S2, S3 for a complete list of metrics analyzed).

Following porewater extraction, sediment slices (at cm increments) were preserved for microbial analysis (described below), organic matter, and chlorophyll concentration. Organic matter was measured by loss on ignition (following Heiri et al. 2001), and chlorophyll was measured by fluorometry on a Turner Designs model 10-AU fluorimeter (following Holm-Hansen et al. 1965).

Microbial analysis

DNA was extracted from 0.25 to 0.30 g of sediment from the vertically sectioned push core samples with the DNeasy PowerSoil Kit (Qiagen) following manufacturer's instructions. The V4 region of the 16S rRNA gene was PCR-amplified with HotStart Taq Plus MasterMix (Qiagen) in triplicate with 515fb and 806rb primers that were bidirectionally barcoded to facilitate multipl exed sequencing following the Earth Microbiome Protocol (Caporaso et al. 2012; Apprill et al. 2015). Amplicons were

pooled, quantified using a Qubit, and cleaned using the Qiaquick PCR purification kit (Qiagen). Bidirectional sequencing was performed on the Illumina MiSeq platform using the V2 chemistry (2 × 250 bp) at the Center for Quantitative Life Sciences (CQLS) at Oregon State University. The 16S rRNA gene sequences are archived in the National Center for Biotechnology Information public database under accession SRP107137 (https://www.ncbi.nlm.nih.gov/bioproject/PRJNA386387).

16S rRNA gene sequences were quality filtered, aligned, and assigned using the Qiime2 pipeline as described in Thurber et al. (2020) with the pipeline provided in Supporting Information. Amplicon sequence variants (ASVs) were assigned taxonomy using Silva V138 (*see* Supporting Information), and we followed the taxonomic nomenclature within that version. Beta and alpha diversity metrics were determined in Qiime2 and plotted both in Qiime2 and R (Version 1.4.1717) as appropriate. After running Qiime2 analysis on the 16S sequences, the PiCRUST2 extension for Qiime2 was used to generate predicted KEGG pathways, using the standard parameters. The list of predicted KOs was incorporated into further analyses. ASV tables were analyzed in PRIMER7, and statistical analysis, including ANOSIM and DistLM, was performed on the ASVs. ANOSIM allowed testing of the significance of between-group differences associated with our hypothesis, while DistLM explored the explanatory power of environmental variables. PiCRUST2 and ASV data were interpreted within R to visualize patterns in environmental gradients, geochemistry, ASVs, and KO abundance. The heatmap function in R's stats package, as well as the R packages phyloseq and ggplot, were used to create figures and perform statistical analysis. This includes NMDS plots using Bray–Curtis distance calculations generated from the ASV tables. Selected KO identifiers representing genes relevant to methane, nitrogen, and sulfur metabolism were also highlighted.

Results

Ecosystem structure across the margin environment

Qualitative habitat structuring along water depth gradients

We observed heterogeneity across all seep ecosystems, with water depth appearing to be a structuring feature across the three regions (Fig. 2; Supporting Information Table S1).

i. The three shallow (< 200 m) sites (AC190, HC100, and CQ150) had no observable seep megafauna nor exposed carbonates, with the only indications of seepage being sparse microbial mats and patches of reduced sediment, along with small "bubble-bursts" from the seafloor.
ii. At the three mid-depth (450–650 m) locations (AC500, HC500, and CQ620), carbonate platforms extend across the sites below a shallow sediment layer, with some of these carbonates protruding above the sediment surface (notably at CQ650). Extensive clam beds were found along with patchy microbial mats and reduced sediments. A large field of bubble plumes was seen at AC500, and sporadic bubble plumes were recorded at the other mid-depth sites.
iii. At the apparent center of seep activity of the two sites that intersected the oxygen minima of the prevailing OMZ (CQ750 and AC800), there were prevalent pockmarks, reduced sediments, and microbial mats on the seafloor. There were no observable seep fauna or exposed carbonates in the seep center. However, clams and carbonates were seen on the periphery of the CQ750 seep. Seepage in the periphery did not appear as intense as in the core of this site, with no characteristic reduced sediments, microbial mats, or pockmarks.
iv. At the three deeper (> 1000 m) locations (AC1350, HC1250, and CQ1400), abundant seep characteristic

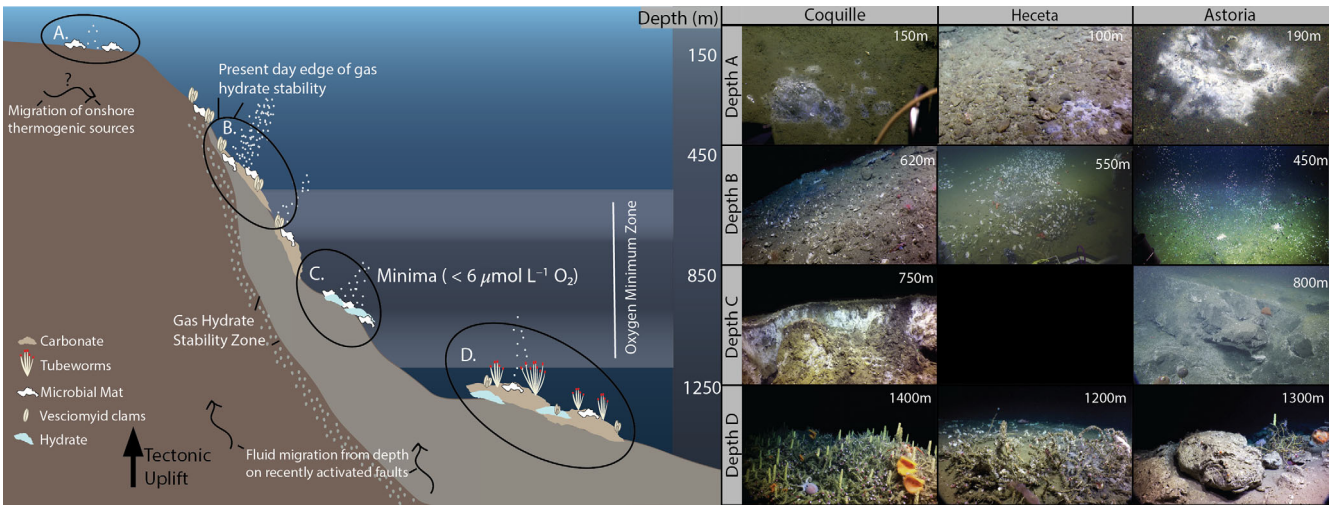

Fig. 2. Schematic of the occurrence of marine methane seeps included in this study from the Cascadia Margin. Representative photos from each site are provided, with a correlation to the indicated depth groupings. The small black arrows indicate either the migration of fluids from depth on recently activated faults (upwards arrows), or the potential migration of onshore thermogenic sources (horizontal seaward arrows; e.g., Torres et al. 2009).

features were observed. Extensive clam beds and microbial mats covered the seafloor. Large and dense vestimentiferan tubeworm bushes were present and carbonate structures and boulders were also common, resulting in a high structural seafloor rugosity. Exposed gas hydrate was observed at HC1250 along with apparent pockmarks and intermittent bubble streams.

Geochemical gradients along the margin

Bottom water oxygen concentrations varied across sites (Supporting Information Table S1), with the highest concentrations found at the shallow sites (54.4–86.3 μmol L^{-1}), declining toward our mid-depth sites (10.0–20.1 μmol L^{-1}) to a minima at the core of the OMZ (4.9–5.1 μmol L^{-1}) and then increasing with depth to our deeper sites (13.5–25.7 μmol L^{-1}). Sediment geochemical parameters were not available consistently across all sites, but, when available, notable variability was observed (Fig. 3; Supporting Information Tables S2, S3). Elevations in sediment organic matter and chlorophyll *a* (Chl *a*) pigments include high organic matter at the oxygen minima site AC800 (14.4% compared to an average of 8.4%) and high Chl *a* concentrations at sites CQ620 and CQ730 (7.8 and 8.0 μg mg^{-3}, respectively, compared to an average of 3.9 μg mg^{-3}). The lowest Chl *a* concentrations were observed at the Astoria Canyon deep site (AC1350; 6.0% organic matter and 1.6 μg mg^{-3} Chl *a*) and the Coquille shallow site (CQ150; 3.5% organic matter and 3.1 μg mg^{-3} Chl *a*). The porewater concentrations of methane, sulfide, and sulfate (Fig. 3; Supporting Information Table S2), as well as other geochemical parameters, including trace metals, (Supporting Information Table S3), were highly variable across sites and habitat types.

General trends in microbial communities across sites

The microbial community was characterized with > 2800 sequences of the V4 region of the 16S rRNA gene per sample, after quality control. On average, 7% of all recovered sequences belonged to Archaea and 91% to Bacteria. Samples from microbial mats had the highest percentage of Archaea (9% of sequences on average), with nearby non-seep sediments having the lowest (3%).

A total of nine Bacterial phyla dominated 77% of total sequences, with remaining phyla rare (< 1%) within the overall microbial community (Fig. 3). Proteobacteria comprised 52% of sequences, followed by Bacterioidetes (7%), Epsilonbacteraeota (6%), Chloroflexi (6%), Plantocymeycetes (4%), Acidobacteria (2%), Atribacteria (1%), and Actinobacteria (1%). Few differences were seen between habitat types, although Epsilonbacteraota and Atribacteria, rare in nearby

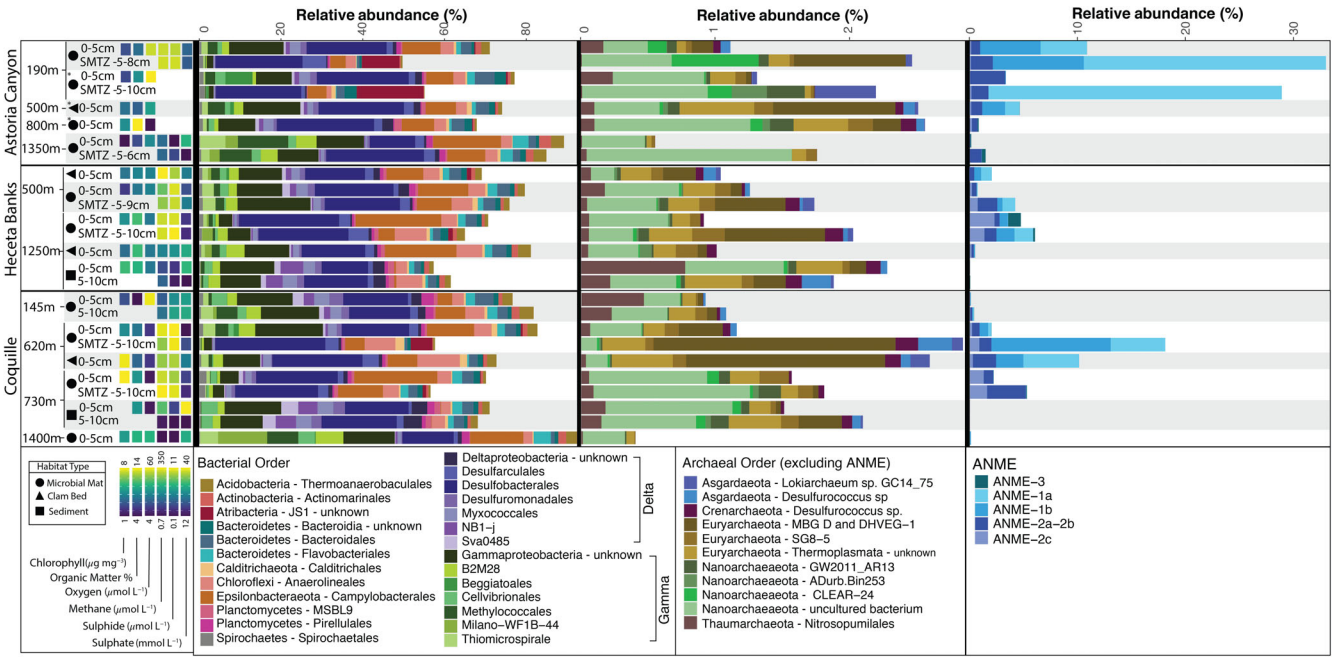

Fig. 3. Geochemical characteristics and microbial community relative abundances across all sites, grouped by region and subdivided by depth range. Samples are averaged by vertical depth in sediment (e.g., 0–5, 5–10 cm), sulfate methane transition zones (SMTZs; as indicated by geochemical downcore data) are indicated when present, and habitat type is provided (e.g., microbial mat vs. clam bed). Boxes on the left-hand side show geochemical characteristics associated with the microbial relative abundances on the right-hand side. Geochemical characteristics include chlorophyll and organic matter from sediment cores as well as methane, sulfide, and sulfate data from porewater extracted from the sediment cores. Oxygen data from water column measurements 0.5 m above the seafloor was also provided. Corresponding raw geochemical data is provided in Supporting Information Table S2. The microbial community, from the sediment cores, is divided into Bacterial and Archaeal orders, with ANME taxa separated for visualization purposes.

non-seep sediments (0.2% and 0.03%, respectively), were more prevalent in seep sediments (7% and 2%, respectively). Euryarchaeota was the most dominant Archaeal phylum throughout, followed by Nanoarchaeota—the remaining Archaeal phyla comprised less than 1% of total sequences.

The Proteobacteria that dominated these sequences were largely attributed to two classes, Deltaproteobacteria (25%) and Gammaproteobacteria (22%). Camplyobacteria, Bacteroidia, and Anaerolinaea classes were also abundant across most samples (> 1%). Methanomicrobia was the only Archaeal class to comprise more than 1% of total sequences.

The most dominant bacterial orders were Desulfobacterales (16%) and unknown Gammaproteobacteria (8%) across all samples. Campylobacterales (9%) was dominant in all microbial mat and clam bed sediments but comprised a rare portion (0.1%) of nearby non-seep sediments. The aerobic methanotrophic Methylococcales was highly variable in abundance across seep samples (ranging from 10% to 0.1%) and negligible in nearby non-seep sediments (0.6%).

Gammaproteobacteria were not limited to the aforementioned unclassified order and others present included B2M28, Cellvibrionales, and Thiomicropsirales, which made up > 1% across all samples. In addition to the most abundant Deltaproteobacterial order, Desulfobacterales, there were also other orders present within this class, including Myxococcales, Desulfarculales, NB1-j, and Desulfuromondales; these groups were all common at > 1%. Other bacterial orders, such as Anaerolineales, Bacteroidales, Thermoanaerobaculales, and Flavobacteriales, were also common (> 1%) across all samples. While ANME-1 was the most dominant archaeal order, this was largely driven by select samples (i.e., AC190) and other notable archaeal orders throughout, including Methanosarcinales (1.2%), unknown Woesarchaeia (0.3%), and Marine Benthic Group D and DHVEG-1 (0.3%).

Microbial variance across sites and environmental conditions

Multiple variables were considered when assessing the structure and distribution of the microbial communities found across the seep sites reported here (Fig. 4). Depth explained the highest proportion of observed variance in the microbial communities, explaining 11% of patterns in beta diversity as well as 15% of alpha diversity patterns (DistLM marginal tests; Supporting Information Tables S4–S7). A clearer correlation between variations in water depth and beta diversity can be seen when we consider only the upper 0–5 cm sediment fraction (Fig. 4b), which avoids the clear influence of redox gradients in lower sediment fractions (Fig. 4a). Depth was also found to be a significant variable in ANOSIM testing, and dissimilarity between depth groupings was strongest between the deep and shallow sites based on ANOSIM (Supporting Information Tables S8, S9). Some orders were notably absent at certain depths (e.g., Desulfarculales was absent at shallow sites),

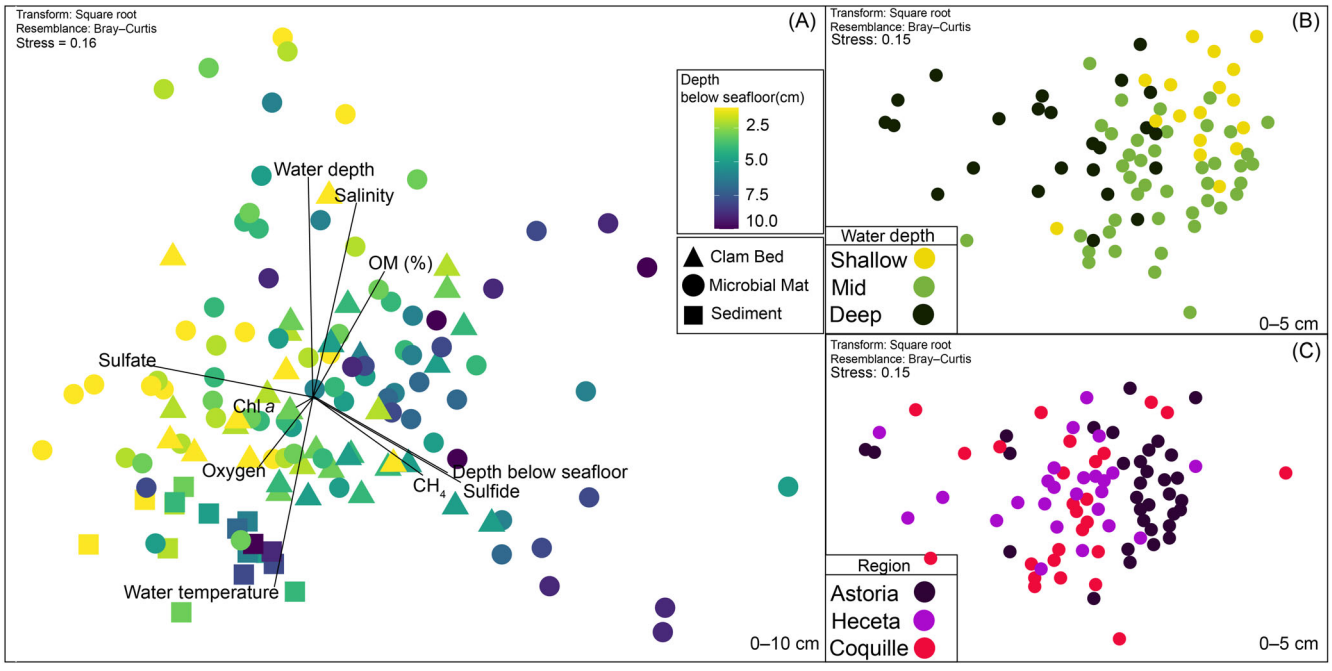

Fig. 4. NMDS plots of Bray–Curtis distance calculations for (**a**) all samples included in the study and (**b**, **c**) only samples within the 0–5 cm sediment fractions. (**a**) Depth below the seafloor of each sample is indicated by the provided color gradient. Habitat is indicated by shape, with sediment (squares) representing samples from "background" sediments that appeared to not be influenced by seep activity. Environmental vectors are fit to the ordination space and represent environmental data from both sediment, sediment porewaters and water column sampling or measurements (as indicated in Fig. 3). (**b**) Ordination of 0–5 cm sediment fractions colored by depth. (**c**) Ordination of 0–5 cm sediment fractions colored by region.

and similarly, certain taxa appeared differentially abundant within specified depth groupings (e.g., Milano-WF1B-44 predominantly found within deep sites; SIMPER analysis; Supporting Information Table S10).

Changes in depth often covaried with changes in oxygen concentration (Fig. 2; Supporting Information Table S1); however, the effect of oxygen and depth in the NMDS ordination space was in opposing directions (Fig. 4). Oxygen was a significant explainer of beta diversity variance based on DistLM analysis, but only explained 3.9% of the variance (Supporting Information Tables S4, S5). Oxygen was a significant driver of differences between samples based on ANOSIM analysis, but varied dissimilarities were seen between oxygen categories (Supporting Information Tables S8, S11). The effect of water depth on the ordination of ASV assignment was in the same direction as the effect of salinity and organic matter percent (Fig. 4), but only organic matter was also a significant explainer of patterns in beta diversity, explaining 4.3% of the variance (Supporting Information Table S4).

Samples did not cluster as clearly by region even when just considering the shallower sediment fractions (Fig. 4c). From a spatial and categorical analysis (ANOSIM), only the Heceta Banks and Astoria Canyon regions were significantly different from each other (Supporting Information Table S12). Latitude was not a significant variable for explaining patterns of beta diversity or alpha diversity in DistLM testing (Supporting Information Tables S4–S7).

Considering ASV assignments across all samples, the influence of habitat is indicated with non-seep sediments clustering closely together, contrasting with clam bed and microbial mat samples, which are more distributed (Fig. 4). Habitat type was a significant variable when partitioning variance to the various patterns and explained 7.5% of the variance observed in beta diversity (DistLM analysis; Supporting Information Table S4); however, ANOSIM analysis indicated that while both microbial mat and clam bed samples were significantly different from non-seep sediment samples, they were not significantly different from each other (Supporting Information Table S13). The abundance of Camplyobacterales in the microbial mat and clam bed samples was notably differential when compared with non-seep sediments, while NB1-j and Sva0485 were distinguishing taxa in non-seep sediments (based on SIMPER analysis; Supporting Information Table S14).

Clustering by vertical depth below the sediment surface was also apparent (Fig. 4), with this supported by significant differences in DistLM analyses (Supporting Information Tables S4, S5). Methane and sulfide concentrations and the depth below the seafloor strongly fit with the direction of the ordination of deeper sediment fractions of microbial mat samples, while the direction of sulfate and oxygen concentration effects aligned more strongly with shallower fractions. Overall, downcore profiles displayed high variability among sites, even within those collected at similar water depths or habitat types (Supporting Information Figs. S1–S5). However, close associations were seen between sediment geochemistry, predicted gene functions, and indicator microbial taxa. Peaks in methane concentration often corresponded to a drop in sulfate and increases in sulfide, the *mcrA* gene (anaerobic methanotrophy or methanogensis), and various ANME types. Samples from within SMTZs were distinguished from samples outside of the SMTZ in SIMPER analysis with influential taxa, including ANME-1 and JS1, more dominant within SMTZs (Supporting Information Table S15). The SMTZs were highly variable in sediment depth, strength (e.g., concentration of methane/sulfide, abundance of relevant taxa), and characteristics.

Discussion

Cascadia Margin seep microbiomes in the context of global patterns and paradigms

While many of the microbial taxa that are ascribed to the "global seep microbiome" were found across the sites reported here, there was a notable uniqueness both within sites and between sites. Much of the variability that has been reported in seep microbiomes to date has been attributed to differences in bottom-up controls (e.g., methane flux); however, here we see the potential influence of other environmental variables (e.g., depth, overlying oxygen concentrations, and organic matter concentrations) in shaping microbial communities at seep sites. While the phylum's Atribacteria and Epsilonbacteraota have not been highlighted as core members of global seep microbiomes (Ruff et al. 2015), they have been commonly found at seep sites, and are seen throughout the samples presented here. Atribacteria ASVs were dominated by an unknown genus of the order JS-1 and were more common in deeper sediment fractions within or below the SMTZ. Often found in high abundance in deep subsurface biospheres, JS-1 Atribacteria have been found elevated in hydrate-bearing sediments in the region (Glass et al. 2021) and elsewhere (Ruff et al. 2015; Marlow et al. 2021), and have been shown capable of entering seep habitats through upward advection with fluid flow (Hoshino et al. 2017). A high proportion of Epsilonbacteraota ASVs within seep samples were the Campylobacterales genus Sulfurovum, a non-mat forming sulfide-oxidizing bacteria that has been found in abundance at other seeps in the region (Marlow et al. 2014; Seabrook et al. 2018).

There was a high relative abundance of other taxa that are not frequently considered core components of a methane seep microbiome. Anaerolineales (in the phylum Chloroflexi), Bacteroidales, and an unknown Bacteroidia (both in the phylum Bacteroidetes) in addition to MSBL-9 and Pirellulaes (both in the phylum Planctomycetes) were all notable members of the seep microbial community. While their role in methane seep microbiomes remains rather elusive, these taxa have been observed in high abundance in other seep environments (Seabrook et al. 2018; Marlow et al. 2021) and are considered

heterotrophs potentially involved in hydrocarbon metabolism (Sherry et al. 2013). Bacteroidales and the class Bacteroidia may be involved in hydrocarbon degradation at seeps (e.g., Miller et al. 2019). The Planctomycetes MSBL-9 has been associated with anoxic, hypersaline cold seeps (Maignien et al. 2013) and Pirellulales are associated with nitrification and denitrification in subsaturated oxygenated conditions (Cohen et al. 2021).

While ANME has often been associated with sulfate-reducing bacterial partners, they can also form partnerships with iron and manganese reducers, and nitrogen fixation genes are present within ANME aggregates (Beal et al. 2009; Dekas et al. 2014). Here, we saw close coupling between predicted genes for anaerobic methane oxidation and nitrogen fixation as a key pattern within the seep (Dekas et al. 2014); however, targeted omics approaches are needed to confirm this predictive pattern. Denitrification and sulfide oxidation genes closely followed each other in vertical profiles of some sediment cores as well. Denitrification coupled to anaerobic methane oxidation has been indicated as a potentially important pathway in seep settings (Jing et al. 2020), and the coupling of sulfide oxidation with denitrification has been seen in industrial settings and at hydrothermal vents as a route to remove hydrogen sulfide from a system (Trembath-Reichert et al. 2019).

Drivers of variability across the margin environment

Clear depth gradients were seen in the overall structure of seep habitats on the Cascadia Margin described here, including both the microbial community structure and the qualitative observations of seep-endemic megafauna present. We posit that the heterogeneity observed on the Cascadia Margin results from a myriad of different interacting processes, including the significant role of environmental variables in shaping the community structure at seep sites, which in some cases may imprint over methane flux variability. This makes assignment of a given parameter to a specific ecosystem response very challenging. For example, increasing water depth coincides with less surface production and shifts in geologic and oceanographic settings. Our results indicate that multiple depth-correlated processes act together to create unique seep communities along depth gradients throughout the Cascadia Margin (Fig. 5). These include competition of chemosynthetic production with (1) photosynthetic/surface production; (2) bottom water oxygen gradients; (3) geologic, oceanographic, and fluid flow dynamics; and (4) seep episodicity. Many of these provide a glimpse into the many variables impacting seep structure and successional stages, as discussed below.

Influence of surface production

The deposition of surface production can provide a significant energy source that, in high enough concentrations, can obscure the extent of the influence of a seep. Competition (i.e., from photosynthetic production) can limit the growth of seep-specific animals and microbes (Sahling et al. 2003; Römer et al. 2014). In shallow seeps, the transitional gradient, or ecotone, that extends away from a seepage site has been reported to be sharper and smaller than deeper sites—an effect attributed to shallower sites having a larger photosynthetic input resulting in a heterotrophic rather than in situ autotrophic community. Indeed, the only seep fauna observed at the shallow sites in this study were patchy microbial mats.

While our observation of no symbiont-bearing megafauna (e.g., vesicomyid clams, bathymodiolin mussels, and siboglinid tubeworms) at seeps shallower than 200 m water depth was qualitative, this is an effect well supported in the literature. Previous studies have suggested the exclusion of symbiont-bearing megafauna at these shallow seep sites is due to the increased abundance of predators at shallower depths and/or increased photosynthetic input (Sahling et al. 2003; Römer et al. 2014). Intriguingly, this depth-related effect on seep-endemic megafauna does not appear to extend to the core seep microbiome in our study. Despite the sparse microbial mats and no observable seep megafauna at the shallow sites studied here, the communities present were rich with seep-associated microbes. In fact, the highest abundance of ANME (over 30% of the overall community) seen among all sites was seen at the shallow Astoria Canyon site (AC190). This suggests that metazoan competition, likely driven by energy availability and potential quality, is divested from microbial structures and leads to this pattern.

Interactions with oxygen gradients

OMZs can be deterministic on the distribution of biological communities on margins. For example, mega-, macro-, and meiofauna have been shown to have decreased abundance and diversity within OMZs (e.g., Sellanes et al. 2010; Bryant et al. 2012). This impact is not limited to metazoan taxa as microbial phylogenetic and trait diversity has been shown to decrease in OMZs (Bryant et al. 2012), with active research quantifying microbially facilitated functions (i.e., nitrogen fixation) in pelagic and benthic OMZ ecosystems (e.g., Bandekar et al. 2018). OMZs do not have a unidirectional impact on seep environments, though, with local factors, including sulfide concentrations and fluid flow, being important for shaping the communities as well as oxygen (Levin et al. 2010; Guilini et al. 2012).

In this study, oxygen concentrations covaried with patterns in microbial community structure; however, water depth, habitat type depth within the sediment, organic matter loading, and the concentration of methane and sulfate appeared more significant. We note the absence of ANME-1 in the OMZ sites, despite being common at other seep locations in the region, and the higher relative abundance of ANME-2; while this is notable there is not necessarily a causative link. While certain microbial taxa (e.g., NC10 and ANME-2d) and functions (e.g., anammox and increased coupling of nitrate reduction to methane oxidation) have been seen at other OMZ sites, we

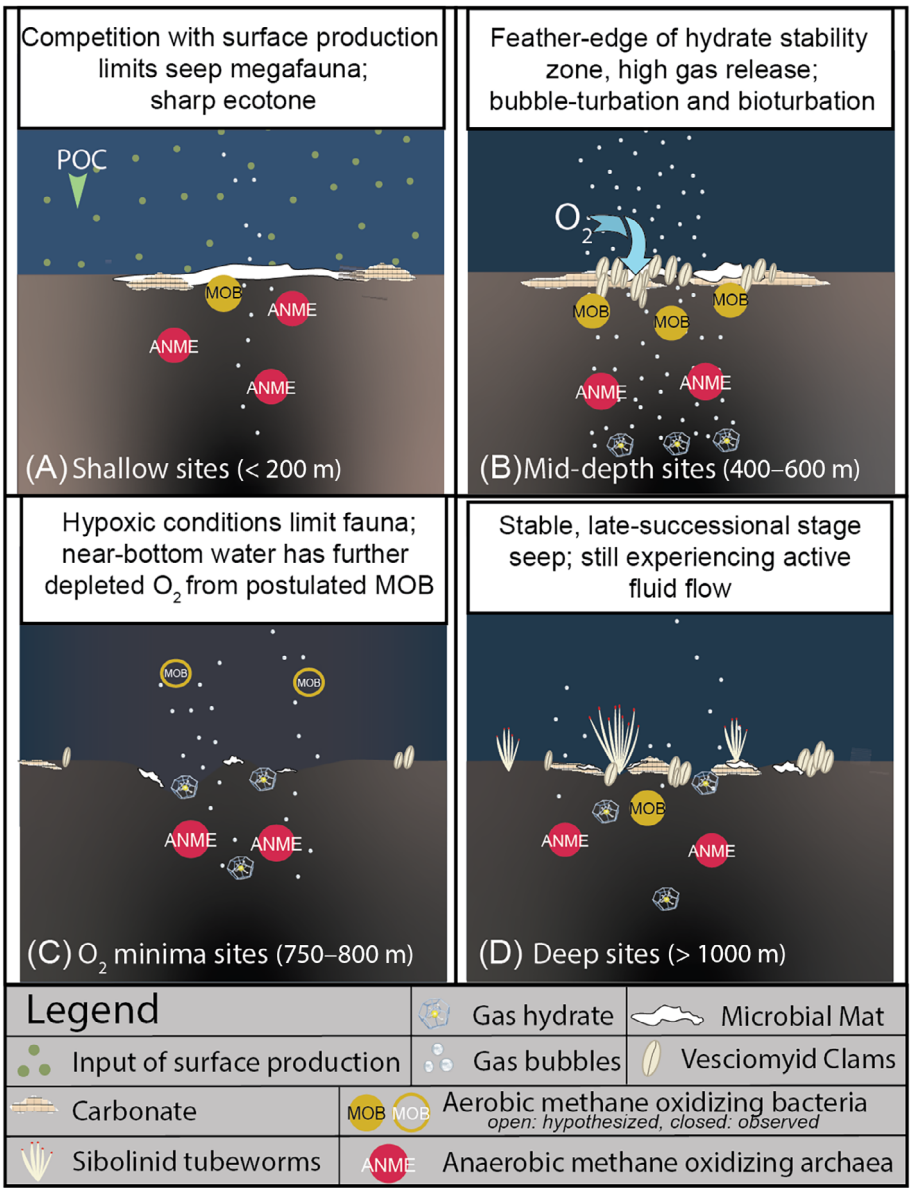

Fig. 5. Schematic of the hypothesized dominant influencing variables discussed within the text for each major depth grouping. (**a**) In shallow sites (< 200 m), competition with surface production limits the development of seep megafauna and a sharp ecotone between seep and non-seep environment is observed. ANME and MOB are common. (**b**) At the feather edge of hydrate stability, bubble-turbation and bioturbation oxygenate deeper sediment layers, pushing the sulfate methane transition zone (SMTZ) below what is measured in our samples and leading to an abundance of aerobic methanotrophs throughout sampled cores. (**c**) Within the minima of the oxygen minimum zone (OMZ), hypoxic conditions limit seep megafauna, with this potentially exacerbated by methane oxidation in the water column further drawing down oxygen concentrations. (**d**) Geologically stable conditions create late-successional stage seeps, with abundant seep megafauna and carbonates.

did not observe an abundance of those taxa here (Thamdrup et al. 2021). Although Planctomycetes, associated with anammox, were observed, they were not elevated at the OMZ sites and predictive gene analysis did not reveal the presence of anammox-related genes.

The impact of oxygen availability on the distribution of microbes in OMZs may be obscured in highly reducing environments such as seeps. In these habitats subsurface fluid flow can shift redox gradients over a scale that is more critical to microbial niches, where hypoxia to near anoxia is normal even within mm of the surface sediment. This is in line with observations across seeps for other faunal groups suggesting that other factors, including the impact of variable fluid flow, may be driving the structure and distribution of the communities, at least within the sediment (e.g., Levin et al. 2010). The impact of oxygen availability on the distribution of seep megafauna, however, may be more apparent.

The apparent reduced prevalence of vesicomyids observed in the seep center of the oxygen minima sites could indicate a low-oxygen limitation that is reached nearer to the seep center of the OMZ minima, where seep activity could be further depleting the oxygen concentration in the benthic boundary layer that the animals inhabit (e.g., Boetius and Wenzhöfer 2013). However, the driving factors in siboglinid distribution are potentially more complex. In line with previous work along the Cascadia Margin, we observed no siboglinid tubeworms shallower than 1000 m across all sites (Seabrook et al. 2018). While it is conceivable that the hypoxic conditions within the oxygen minima of the OMZ in Cascadia may limit siboglinids in this zone, there are also no siboglinid assemblages at the mid-depth (490–620 m) sites despite having similar bottom water oxygen concentration to the Cascadia deep sites (> 1000 m deep). In addition, these taxa have been observed occurring in this mid-depth range in other global locations (e.g., at the 540 m water depth seep at Bush Hill in the Gulf of Mexico; MacDonald et al. 1989). We suggest that the distribution of siboglinid on the Cascadia Margin may more broadly be limited by impacts of the prevailing OMZ on factors such as larval recruitment and connectivity across the margin; however, future work would be required to explore this.

Similarly, the consistent absence of mytilid mussels across the Cascadia Margin in all studies undertaken to date in the region is notable. We suggest that the prevailing OMZ could similarly be deterministic in this widespread absence. Mytilid mussels have been shown to have double the respiration rate of vesicomyid clams (33 μmol g^{-1} dry weight h^{-1} compared to 16.1 μmol g^{-1} dry weight h^{-1}, respectively), largely attributed to the commensal scaleworm in the mytilids (Khripounoff et al. 2017). This higher respiration rate of mytilid mussels could limit their development in methane seeps on the more oxygen-limited Cascadia Margin, as well as potential interactions of the OMZ on larval dispersal, similar to what we suggest with the siboglinid tubeworms. The differences in distribution between siboglinids and vesicomyid clam beds, and the notable absence of mytilid mussels on the Cascadia Margin, may provide a meaningful insight into connectivity and factors driving seep megafauna dispersal patterns in the region, which could potentially be explored with targeted eDNA studies of relevant larvae around the region (e.g., Hilário et al. 2015).

Influence of geologic, oceanographic, and fluid flow dynamics

The depth-related variances in seep ecosystems observed here across the Cascadia Margin co-occur with prevailing variations in geologic and hydrographic regimes. Oceanographic conditions impact primary productivity and bottom oxygen concentrations across the Cascadia Margin, where methane seep ecosystems also intersect a geologic setting characterized by accretion of thick Pleistocene Astoria and Nitinat fan sediments. The well-known expulsion of hydrocarbon-bearing fluids on this, and other active continental margins, is driven by dehydration and compaction of the sediment column during accretionary wedge development. Analyses of gas venting from seeps have been shown to be dominated by methane (Baumberger et al. 2018 *and within*). The relative contributions of biogenic vs. thermogenic sources, as well as the role of mixing and oxidation processes, act in concert to generate variations in the molecular and isotopic composition of the venting hydrocarbons, which cannot be directly attributed to depth or location along the margin (Baumberger et al. 2018), and could contribute to variations in the microbial community (Orcutt et al. 2010).

Investigations have also provided insights into different fluid and gas migration pathways and the factors that modulate gas discharge, including spatial variations, along the margin. Since the earliest Cascadia Margin investigations, methane discharge at cold seeps was known to be co-located with the low wedge taper and widely spaced accretionary thrusts that characterize the broad accretionary prism off Washington and northern Oregon. The co-location with surface expressions of these faults is particularly evident in the deeper sites, originally referred to as the First Accretionary Ridge (Suess et al. 1985). These well-defined faults channel methane-bearing fluids to the seafloor at the deeper, apparently later successional stage, seep sites described in this study.

Methane discharge in the Second Accretionary Ridge, now known as Hydrate Ridge (~ 800 m water depth), exhibits a wider range of episodicities, from tidal modulations on the Northern Hydrate Ridge (Torres et al. 2002) seeps, to decadal (30–50 yr) transient fluid flow at southern Hydrate Ridge, in response to pressure fluctuations in the gas reservoir underlying the regional hydrate stability zone at the southern Hydrate Ridge (Daigle et al. 2011). Here, methane is thought to migrate along a stratigraphically defined coarse sediment conduit and by pressure-driven hydrofracturing (Tréhu et al. 2004*a*; Daigle et al. 2011). On longer timescales, Bangs et al. (2005) document methane pulses associated with gas hydrate dynamics on glacial–interglacial periodicity. In addition to these drivers of flow, earthquakes have been shown to trigger methane release in other margins (Fischer et al. 2013), and given the level of seismic activity in Cascadia, it is likely that earthquake activity also contributes to modulating methane fluxes. Such variances in fluid routing mechanisms and methane flux episodicity can impact the diversity of the microbial community present at the seep site, through mechanisms such as the advection-assisted transport of deep biosphere microbes to shallow seep sediment systems at some sites (Chakraborty et al. 2020) or variances in the fluid and gases seeping at the site impacting the microbial community present (Vigneron et al. 2017).

Among the various variables related to geologic influences, perhaps the most widely invoked is the formation and dissociation of gas hydrate. Mid-depth seeps studied here occur

toward the upper featheredge of the gas hydrate stability zone, which in this margin is found at approximately 500 m water depth (Johnson et al. 2015; Baumberger et al. 2018). At this critical depth, subtle shifts in pressure and temperature can modulate the release of free gas from these gas hydrate reservoirs (Torres et al. 2009; Baumberger et al. 2018). Extensive and vigorous bubbling was often encountered at sites AC500 and HB500, supporting past suggestions that widespread gas hydrate dissociation at this featheredge fuels highly advective methane flux (Johnson et al. 2015; Baumberger et al. 2018). Geochemical data is only available for site HB500, but samples from a clam bed habitat at this site had the highest methane concentrations observed across all sites. This observation should be taken as a minimum value given the fact that obtaining methane concentration values at sites with methane supersaturations is not possible with conventional coring techniques as samples degas significantly on their way to the ocean surface.

Microbial community analyses at AC500 and HB500, suggest that anaerobic methane oxidation is not a dominant process throughout most of the cores, with ANME types and predicted *mcrA* genes lower in abundance than other sites (e.g., AC190) with similarly elevated methane concentrations. In contrast, aerobic methane oxidation by *Methylomonacea*, also indicated with elevated *pmoA* gene abundance, is more common within the cores. This perceived anomaly may be the result of significant bubble-turbation (vigorous bubbling disturbing redox gradients; Seabrook et al. 2018) and bioturbation by megafauna (Sahling et al. 2002) in aerating sediments enough to restrict anaerobic methane oxidation. Bioturbation and irrigation can shift microbial community perturbations toward aerobic methane oxidation leading to high flux at methane seeps where significant macrofauna colonizes the seafloor (Thurber et al. 2013), and our results at AC500 and HB500 point to this intriguing possibility.

Notably, while gas hydrate disassociation is likely to be occurring at this feathered edge of the gas hydrate stability zone (FEGHS; Baumberger et al. 2018; Merle et al. 2021), the extensive carbonate pavements we observed at these sites indicate that methane discharge is not a recent anthropogenically driven occurrence at these depths, as has been previously invoked (Johnson et al. 2015). More significant, perhaps, may be the temporal shifts in fluid flow and associated gas release that would occur at the FEGHS as the margin experiences changes in bottom water conditions and subduction-related uplift over geologic timescales. Such change could include anthropogenic warming of the bottom water, which has been observed in the region (Hautala et al. 2014) and may induce variations in the rate of methane release as has been observed elsewhere (Ketzer et al. 2020). While methane has been released here for a long period of time, the rate and dynamics are likely driven by a combination of processes occurring across a geologic time scale and those that can be influenced by human activities.

Methane episodicity in shaping seep structure

Methane supply at seep sites experience fluctuations at many timescales. These methane fluctuations encompass tidal (Torres et al. 2002; Römer et al. 2016), seasonal (Ferré et al. 2020; Dølven et al. 2022), and climatic (Ruppel and Kessler 2017; Skarke et al. 2014; Sultan et al. 2020) changes as well as methane reservoir dynamics that can operate in decade-long (Daigle et al. 2011) to geologic (Baumberger et al. 2018; Himmler et al. 2019) timescales. Except for the recent time-series data from seafloor observatories (Römer et al. 2016), discrete samples or observations at a seep community represent a snap-shot view of the habitat, that is, a time-slice of the episodic variability that undoubtedly occurs over time at the site. A recent analysis coupling molecular, geochemical, and numerical approaches using data and samples collected over various seeps offshore Svalbard by Klasek et al. (2021) demonstrates a tightly coupled microbial response to shifting methane fluxes among seeps in various stages, ranging from well-established steady-state conditions to various transitional stages.

The high variability we observe across vertical sediment profiles likely reflects the influence of these many episodic variables. Indications of past methane flux conditions are apparent (Supporting Information Fig. S1A), where sulfate is depleted by 50% and sulfide is elevated, but methane concentrations are low and the methanotrophic abundance is minimal. Apparent active methane flux conditions at the time of sampling (Supporting Information Fig. S1B) occur where the sulfate decrease is nicely coupled to sulfide accumulation and with an elevated methanotrophic community. Non-steady-state conditions with potentially rapidly pulsing methane flow (Supporting Information Fig. S1C) could occur where multiple peaks of methanotrophs are seen throughout the core, but sulfate depletion tied to sulfide accumulation continues below the depth of the core may also suggest a deep SMTZ and presently decreasing methane flux. While our sampling resolution is not enough to fully resolve the episodicity in such a highly variable system, the variation that we see is still notable. None of the sampled seep sites appears characteristic of a steady state; the magnitude and timing of the methane flux appear different across all cores, and each microbial community seems to be responding to different states of perturbation. However, it is intriguing to consider that episodicity could be an inherent part of the steady state at marine methane seeps. To explain the biodiversity of chemosynthetic ecosystems, perhaps a similarly diverse range of varying influences should be considered, from episodicity in methane flux to variables such as seasonality in OMZ distribution or even the episodic deposition of POC on the seafloor.

Conclusion

As climate change impacts threaten food delivery to the deep from surface production, nutrient cycles become altered

by eutrophication and changing land–sea–atmosphere dynamics, and OMZs build in size and persistence the role of environmental variance in shaping the structure and function of methane seep ecosystems become ever more important and intriguing.

Depth is a clear driver of variance in seep microbial communities of the Cascadia Margin; however, the many, varied environmental variables that covary with depth appear deterministic in the trends observed. The combined roles of primary productivity and water depth determine the organic carbon flux to the seafloor, while varied geologic regimes impact fluid and gas delivery and hydrographic regimes drive change through, most notably, the prevailing OMZ in the region. Considering our observations of the varied structure of seep habitats described here, we posit that dissolved oxygen may be deterministic in limiting the distribution of seep fauna on the margin, such as with the apparent depth limitation of siboglinids to depths below 1000 m. The apparent influence seen here of the persistent OMZ on the dispersal of seep-endemic animals is notable and should be considered as a potential ramification of the expansion of OMZs under future climate change scenarios.

Our work highlights the multifaceted aspects that drive community composition beyond localized methane flux and depth, where environmental diversity adds to margin biodiversity in seep systems. The heterogeneity that we see in seep habitats and microbial communities across the Cascadia Margin points to potentially meaningful differences in ecosystem function that we are yet to fully understand. As the regions in which methane seeps occur (and methane seeps themselves) are increasingly targeted or considered for exploitation it is essential that we understand inherent variabilities and sensitives to change.

Data availability statement

All data included within the manuscript is available either within the main text or Supporting Information, or will be provided upon request to the corresponding author.

References

Apprill, A., S. McNally, R. Parsons, and Weber, L. 2015. Minor revision to V4 region SSU rRNA 806R gene primer greatly increases detection of SAR11 bacterioplankton. Aquatic Microbial Ecol. **75**: 129–137. doi:10.3354/ame01753

Bandekar, M., N. Ramaiah, and R. M. Meena. 2018. Diversity and abundance of denitrifying and anammox bacteria from the Arabian Sea oxygen minimum zone. Deep-Sea Res. II: Top. Stud. Oceanogr. **156**: 19–26. doi:10.1016/j.dsr2.2018.08.008

Bangs, N. L. B., R. J. Musgrave, and A. M. Tréhu. 2005. Upward shifts in the southern Hydrate Ridge gas hydrate stability zone following postglacial warming, offshore Oregon. J. Geophys. Res.: Solid Earth **110**: B03102. doi:10.1029/2004JB003293

Baumberger, T., R. W. Embley, S. G. Merle, M. D. Lilley, N. A. Raineault, and J. E. Lupton. 2018. Mantle-derived helium and multiple methane sources in gas bubbles of cold seeps along the Cascadia Continental Margin. Geochem. Geophys. Geosyst. **19**: 4476–4486. doi:10.1029/2018GC007859

Beal, E. J., C. H. House, and V. J. Orphan. 2009. Manganese- and iron-dependent marine methane oxidation. Science **325**: 184–187. doi:10.1126/science.1169984

Boetius, A., and F. Wenzhöfer. 2013. Seafloor oxygen consumption fuelled by methane from cold seeps. Nat. Geosci. **6**: 725–734. doi:10.1038/ngeo1926

Bryant, J. A., F. J. Stewart, J. M. Eppley, and E. F. DeLong. 2012. Microbial community phylogenetic and trait diversity declines with depth in a marine oxygen minimum zone. Ecology **93**: 1659–1673. doi:10.1890/11-1204.1

Caporaso, J. G., and others. 2012. Ultra-high-throughput microbial community analysis on the Illumina HiSeq and MiSeq platforms. ISME J. **6**: 1621–1624. doi:10.1038/ismej.2012.8

Chakraborty, A., and others. 2020. Hydrocarbon seepage in the deep seabed links subsurface and seafloor biospheres. Proc. Natl. Acad. Sci. USA **117**: 11029–11037. doi:10.1073/pnas.2002289117

Claypool, G. E., and I. R. Kaplan. 1974. The origin and distribution of methane in marine sediments, p. 99–139. *In* I. R. Kaplan [ed.], Natural gases in marine sediments. Springer. doi:10.1007/978-1-4684-2757-8_8

Cohen, A. B., and others. 2021. Particle-associated and free-living microbial assemblages are distinct in a permanently redox-stratified freshwater lake. doi:10.1101/2021.11.24.469905

Cordes, E. E., and others. 2010. The influence of geological, geochemical, and biogenic habitat heterogeneity on seep biodiversity: Seep habitat heterogeneity. Mar. Ecol. **31**: 51–65. doi:10.1111/j.1439-0485.2009.00334.x

Daigle, H., N. L. Bangs, and B. Dugan. 2011. Transient hydraulic fracturing and gas release in methane hydrate settings: A case study from southern Hydrate Ridge. Geochem. Geophys. Geosyst. **12**: Q12022. doi:10.1029/2011GC003841

Dekas, A. E., G. L. Chadwick, M. W. Bowles, S. B. Joye, and V. J. Orphan. 2014. Spatial distribution of nitrogen fixation in methane seep sediment and the role of the ANME archaea: Nitrogen fixation in methane seep sediment. Environ. Microbiol. **16**: 3012–3029. doi:10.1111/1462-2920.12247

Dølven, K. O., B. Ferré, A. Silyakova, P. Jansson, P. Linke, and M. Moser. 2022. Autonomous methane seep site monitoring offshore Western Svalbard: Hourly to seasonal variability and associated oceanographic parameters. Ocean Sci. **18**: 233–254. doi:10.5194/os-18-233-2022

Ferré, B., and others. 2020. Reduced methane seepage from Arctic sediments during cold bottom-water conditions. Nat. Geosci. **13**: 144–148. doi:10.1038/s41561-019-0515-3

Fischer, D., J. M. Mogollón, M. Strasser, T. Pape, G. Bohrmann, N. Fekete, V. Spiess, and S. Kasten. 2013. Subduction zone earthquake as potential trigger of submarine hydrocarbon seepage. Nat. Geosci. **6**: 647–651. doi:10.1038/ngeo1886

Glass, J. B., P. Ranjan, C. B. Kretz, B. L. Nunn, A. M. Johnson, M. Xu, J. McManus, and F. J. Stewart. 2021. Microbial metabolism and adaptations in *Atribacteria*-dominated methane hydrate sediments. Environ. Microbiol. **23**: 4646–4660. doi:10.1111/1462-2920.15656

Goldfinger, C., C. H. Nelson, J. E. Johnson, and The Shipboard Scientific Party. 2003. Holocene earthquake records from the Cascadia subduction zone and northern San Andreas fault based on precise dating of offshore turbidites. Annu. Rev. Earth Planet. Sci. **31**: 555–577. doi:10.1146/annurev.earth.31.100901.141246

Goñi, M. A., J. A. Hatten, R. A. Wheatcroft, and J. C. Borgeld. 2013. Particulate organic matter export by two contrasting small mountainous rivers from the Pacific Northwest, U.S.A. J. Geophys. Res.: Biogeosci. **118**: 112–134. doi:10.1002/jgrg.20024

Gooday, A. J., B. J. Bett, E. Escobar, B. Ingole, L. A. Levin, C. Neira, A. V. Raman, and J. Sellanes. 2010. Habitat heterogeneity and its influence on benthic biodiversity in oxygen minimum zones. Mar. Ecol. **31**: 125–147. doi:10.1111/j.1439-0485.2009.00348.x

Greinert, J., K. B. Lewis, J. Bialas, I. A. Pecher, A. Rowden, D. A. Bowden, M. De Batist, and P. Linke. 2010. Methane seepage along the Hikurangi Margin, New Zealand: Overview of studies in 2006 and 2007 and new evidence from visual, bathymetric and hydroacoustic investigations. Mar. Geol. **272**: 6–25. doi:10.1016/j.margeo.2010.01.017

Grupe, B. M., M. L. Krach, A. L. Pasulka, J. M. Maloney, L. A. Levin, and C. A. Frieder. 2015. Methane seep ecosystem functions and services from a recently discovered southern California seep. Mar. Ecol. **36**: 91–108. doi:10.1111/maec.12243

Guilini, K., L. A. Levin, and A. Vanreusel. 2012. Cold seep and oxygen minimum zone associated sources of margin heterogeneity affect benthic assemblages, diversity and nutrition at the Cascadian margin (NE Pacific Ocean). Prog. Oceanogr. **96**: 77–92. doi:10.1016/j.pocean.2011.10.003

Hautala, S. L., E. A. Solomon, H. P. Johnson, R. N. Harris, and U. K. Miller. 2014. Dissociation of Cascadia margin gas hydrates in response to contemporary ocean warming. Geophys. Res. Lett. **41**: 8486–8494. doi:10.1002/2014GL061606

Heiri, O., A. F. Lotter, and G. Lemcke. 2001. Loss on ignition as a method for estimating organic and carbonate content in sediments: Reproducibility and comparability of results. J. Paleolimnol. **25**: 101–110. doi:10.1023/A:1008119611481

Hilário, A., and others. 2015. Estimating dispersal distance in the deep sea: Challenges and applications to marine reserves. Front. Mar. Sci. **2**: 6. doi:10.3389/fmars.2015.00006

Himmler, T., and others. 2019. A 160,000-year-old history of tectonically controlled methane seepage in the Arctic. Sci. Adv. **5**: eaaw1450. doi:10.1126/sciadv.aaw1450

Holm-Hansen, O., C. J. Lorenzen, R. W. Holmes, and J. D. H. Strickland. 1965. Fluorometric determination of chlorophyll. ICES J. Mar. Sci. **30**: 3–15. doi:10.1093/icesjms/30.1.3

Hoshino, T., T. Toki, A. Ijiri, Y. Morono, H. Machiyama, J. Ashi, K. Okamura, and F. Inagaki. 2017. *Atribacteria* from the subseafloor sedimentary biosphere disperse to the hydrosphere through submarine mud volcanoes. Front. Microbiol. **8**: 1135. doi:10.3389/fmicb.2017.01135

Jing, H., R. Wang, Q. Jiang, Y. Zhang, and X. Peng. 2020. Anaerobic methane oxidation coupled to denitrification is an important potential methane sink in deep-sea cold seeps. Sci. Total Environ. **748**: 142459. doi:10.1016/j.scitotenv.2020.142459

Johnson, H. P., U. K. Miller, M. S. Salmi, and E. A. Solomon. 2015. Analysis of bubble plume distributions to evaluate methane hydrate decomposition on the continental slope. Geochem. Geophys. Geosyst. **16**: 3825–3839. doi:10.1002/2015GC005955

Ketzer, M., and others. 2020. Gas hydrate dissociation linked to contemporary ocean warming in the Southern Hemisphere. Nat. Commun. **11**: 3788. doi:10.1038/s41467-020-17289-z

Khripounoff, A., J. C. Caprais, C. Decker, J. Le Bruchec, P. Noel, and B. Husson. 2017. Respiration of bivalves from three different deep-sea areas: Cold seeps, hydrothermal vents and organic carbon-rich sediments. Deep-Sea Res. II: Top. Stud. Oceanogr. **142**: 233–243. doi:10.1016/j.dsr2.2016.05.023

Klasek, S. A., W.-L. Hong, M. E. Torres, S. Ross, K. Hostetler, A. Portnov, F. Gründger, and F. S. Colwell. 2021. Distinct methane-dependent biogeochemical states in Arctic seafloor gas hydrate mounds. Nat. Commun. **12**: 6296. doi:10.1038/s41467-021-26549-5

Knittel, K., and A. Boetius. 2009. Anaerobic oxidation of methane: Progress with an unknown process. Annu. Rev. Microbiol. **63**: 311–334. doi:10.1146/annurev.micro.61.080706.093130

Kulm, L. D., and others. 1986. Oregon subduction zone: Venting, fauna, and carbonates. Science **231**: 561–566. doi:10.1126/science.231.4738.561

Levin, L. A., and R. H. Michener. 2002. Isotopic evidence for chemosynthesis-based nutrition of macrobenthos: The lightness of being at Pacific methane seeps. Limnol. Oceanogr. **47**: 1336–1345. doi:10.4319/lo.2002.47.5.1336

Levin, L. A., G. F. Mendoza, J. P. Gonzalez, A. R. Thurber, and E. E. Cordes. 2010. Diversity of bathyal macrofauna on the northeastern Pacific margin: The influence of methane seeps and oxygen minimum zones. Mar. Ecol. **31**: 94–110. doi:10.1111/j.1439-0485.2009.00335.x

Levin, L., and others. 2003. Spatial heterogeneity of macrofauna at northern California methane seeps: Influence of sulfide concentration and fluid flow. Mar. Ecol. Prog. Ser. **265**: 123–139. doi:10.3354/meps265123

Levin, L. A., and others. 2016. Hydrothermal vents and methane seeps: Rethinking the sphere of influence. Front. Mar. Sci. **3**: 72. doi:10.3389/fmars.2016.00072

Luff, R., and K. Wallmann. 2003. Fluid flow, methane fluxes, carbonate precipitation and biogeochemical turnover in gas hydrate-bearing sediments at Hydrate Ridge, Cascadia Margin: Numerical modeling and mass balances. Geochim. Cosmochim. Acta **67**: 3403–3421. doi:10.1016/S0016-7037(03)00127-3

MacAvoy, S., R. Carney, C. Fisher, and S. Macko. 2002. Use of chemosynthetic biomass by large, mobile, benthic predators in the Gulf of Mexico. Mar. Ecol. Prog. Ser. **225**: 65–78. doi:10.3354/meps225065

MacDonald, I. R., G. S. Boland, J. S. Baker, J. M. Brooks, M. C. Kennicutt, and R. R. Bidigare. 1989. Gulf of Mexico hydrocarbon seep communities: II. Spatial distribution of seep organisms and hydrocarbons at Bush Hill. Mar. Biol. **101**: 235–247. doi:10.1007/BF00391463

Maignien, L., R. Parkes, B. Cragg, H. Niemann, K. Knittel, S. Coulon, A. Akhmetzhanov, and N. Boon. 2013. Anaerobic oxidation of methane in hypersaline cold seep sediments. FEMS Microbiol. Ecol. **83**: 214–231. doi:10.1111/j.1574-6941.2012.01466.x

Marlow, J. J., J. A. Steele, D. H. Case, S. A. Connon, L. A. Levin, and V. J. Orphan. 2014. Microbial abundance and diversity patterns associated with sediments and carbonates from the methane seep environments of Hydrate Ridge, OR. Front. Mar. Sci. **1**: 44. doi:10.3389/fmars.2014.00044

Marlow, J. J., and others. 2021. Carbonate-hosted microbial communities are prolific and pervasive methane oxidizers at geologically diverse marine methane seep sites. Proc. Natl. Acad. Sci. USA **118**: e2006857118. doi:10.1073/pnas.2006857118

Mau, S., and others. 2017. Widespread methane seepage along the continental margin off Svalbard—From Bjørnøya to Kongsfjorden. Sci. Rep. **7**: 42997. doi:10.1038/srep42997

Merle, S. G., R. W. Embley, H. P. Johnson, T.-K. Lau, B. J. Phrampus, N. A. Raineault, and L. J. Gee. 2021. Distribution of methane plumes on Cascadia Margin and implications for the landward limit of methane hydrate stability. Front. Earth Sci. **9**: 531714. doi:10.3389/feart.2021.531714

Miller, J. I., and others. 2019. Oil hydrocarbon degradation by Caspian Sea microbial communities. Front. Microbiol. **10**: 995. doi:10.3389/fmicb.2019.00995

Niemann, H., and others. 2013. Methane-carbon flow into the benthic food web at cold seeps—A case study from the Costa Rica subduction zone. PLoS One **8**: e74894. doi:10.1371/journal.pone.0074894

Orcutt, B. N., and others. 2010. Impact of natural oil and higher hydrocarbons on microbial diversity, distribution, and activity in Gulf of Mexico cold-seep sediments. Deep-Sea Res. II: Top. Stud. Oceanogr. **57**: 2008–2021. doi:10.1016/j.dsr2.2010.05.014

Paull, C. K., and others. 1984. Biological communities at the Florida escarpment resemble hydrothermal vent taxa. Science **226**: 965–967. doi:10.1126/science.226.4677.965

Riedel, M., M. Scherwath, M. Römer, M. Veloso, M. Heesemann, and G. D. Spence. 2018. Distributed natural gas venting offshore along the Cascadia margin. Nat. Commun. **9**: 3264. doi:10.1038/s41467-018-05736-x

Römer, M., M. Riedel, M. Scherwath, M. Heesemann, and G. D. Spence. 2016. Tidally controlled gas bubble emissions: A comprehensive study using long-term monitoring data from the NEPTUNE cabled observatory offshore Vancouver Island. Geochem. Geophys. Geosyst. **17**: 3797–3814. doi:10.1002/2016GC006528

Römer, M., and others. 2014. First evidence of widespread active methane seepage in the Southern Ocean, off the sub-Antarctic Island of South Georgia. Earth Planet. Sci. Lett. **403**: 166–177. doi:10.1016/j.epsl.2014.06.036

Ruff, S. E., J. F. Biddle, A. P. Teske, K. Knittel, A. Boetius, and A. Ramette. 2015. Global dispersion and local diversification of the methane seep microbiome. Proc. Natl. Acad. Sci. USA **112**: 4015–4020. doi:10.1073/pnas.1421865112

Ruppel, C. D., and J. D. Kessler. 2017. The interaction of climate change and methane hydrates. Rev. Geophys. **55**: 126–168. doi:10.1002/2016RG000534

Sahling, H., D. Rickert, R. W. Lee, P. Linke, and E. Suess. 2002. Macrofaunal community structure and sulfide flux at gas hydrate deposits from the Cascadia convergent margin, NE Pacific. Mar. Ecol. Prog. Ser. **231**: 121–138. doi:10.3354/meps231121

Sahling, H., S. V. Galkin, A. Salyuk, J. Greinert, H. Foerstel, D. Piepenburg, and E. Suess. 2003. Depth-related structure and ecological significance of cold-seep communities—A case study from the Sea of Okhotsk. Deep-Sea Res. I: Oceanogr. Res. Pap. **50**: 1391–1409. doi:10.1016/j.dsr.2003.08.004

Seabrook, S., F. C. De Leo, T. Baumberger, N. Raineault, and A. R. Thurber. 2018. Heterogeneity of methane seep biomes in the Northeast Pacific. Deep-Sea Res. II: Top. Stud. Oceanogr. **150**: 195–209. doi:10.1016/j.dsr2.2017.10.016

Seabrook, S., F. C. De Leo, and A. R. Thurber. 2019. Flipping for food: The use of a methane seep by tanner crabs (*Chionoecetes tanneri*). Front. Mar. Sci. **6**: 43. doi:10.3389/fmars.2019.00043

Sellanes, J., C. Neira, E. Quiroga, and N. Teixido. 2010. Diversity patterns along and across the Chilean margin: A continental slope encompassing oxygen gradients and methane seep benthic habitats. Mar. Ecol. **31**: 111–124. doi:10.1111/j.1439-0485.2009.00332.x

Sherry, A., and others. 2013. Anaerobic biodegradation of crude oil under sulphate-reducing conditions leads to only modest enrichment of recognized sulphate-reducing taxa.

Int. Biodeterior. Biodegradation **81**: 105–113. doi:10.1016/j.ibiod.2012.04.009

Shester, G. G., B. Enticknap, B. Mecum, A. Blacow-Draeger, T. Brock, and S. Murray. 2021. A win-win for deep-sea corals and fishing: Increasing seafloor protections while restoring fishing opportunities off the United States West Coast. Front. Mar. Sci. **7**: 525619. doi:10.3389/fmars.2020.525619

Skarke, A., C. Ruppel, M. Kodis, D. Brothers, and E. Lobecker. 2014. Widespread methane leakage from the sea floor on the northern US Atlantic margin. Nat. Geosci. **7**: 657–661. doi:10.1038/ngeo2232

Sommer, S., and others. 2006. Efficiency of the benthic filter: Biological control of the emission of dissolved methane from sediments containing shallow gas hydrates at Hydrate Ridge. Glob. Biogeochem. Cycles **20**: GB2019. doi:10.1029/2004GB002389

Spitz, Y. H., P. A. Newberger, and J. S. Allen. 2003. Ecosystem response to upwelling off the Oregon coast: Behavior of three nitrogen-based models. J. Geophys. Res.: Oceans **108**: C33062. doi:10.1029/2001JC001181

Suess, E., and others. (1985). Biological communities at vent sites along the subduction zone off Oregon. Bulletin of the Biological Society of Washington. **6**: 475–484.

Sultan, N., A. Plaza-Faverola, S. Vadakkepuliyambatta, S. Buenz, and J. Knies. 2020. Impact of tides and sea-level on deep-sea Arctic methane emissions. Nat. Commun. **11**: 5087. doi:10.1038/s41467-020-18899-3

Thamdrup, B., C. Schauberger, M. Larsen, B. Trouche, L. Maignien, S. Arnaud-Haond, F. Wenzhöfer, and R. N. Glud. 2021. Anammox bacteria drive fixed nitrogen loss in hadal trench sediments. Proc. Natl. Acad. Sci. USA **118**: e2104529118. doi:10.1073/pnas.2104529118

Thurber, A. R., L. A. Levin, A. A. Rowden, S. Sommer, P. Linke, and K. Kröger. 2013. Microbes, macrofauna, and methane: A novel seep community fueled by aerobic methanotrophy. Limnol. Oceanogr. **58**: 1640–1656. doi:10.4319/lo.2013.58.5.1640

Thurber, A. R., S. Seabrook, and R. M. Welsh. 2020. Riddles in the cold: Antarctic endemism and microbial succession impact methane cycling in the Southern Ocean. Proceedings of the Royal Society B: Biological Sciences. **287**: 20201134. doi:10.1098/rspb.2020.1134

Torres, M. E., R. W. Embley, S. G. Merle, A. M. Tréhu, R. W. Collier, E. Suess, and K. U. Heeschen. 2009. Methane sources feeding cold seeps on the shelf and upper continental slope off central Oregon, USA. Geochem. Geophys. Geosyst. **10**: Q11003. doi:10.1029/2009GC002518

Torres, M. E., and others. 2002. Fluid and chemical fluxes in and out of sediments hosting methane hydrate deposits on Hydrate Ridge, OR, I: Hydrological provinces. Earth Planet. Sci. Lett. **201**: 525–540. doi:10.1016/S0012-821X(02)00733-1

Tréhu, A. M., and others. 2004*a*. Feeding methane vents and gas hydrate deposits at south Hydrate Ridge. Geophys. Res. Lett. **31**: L23310. doi:10.1029/2004GL021286

Tréhu, A. M., and others. 2004*b*. Three-dimensional distribution of gas hydrate beneath southern Hydrate Ridge: Constraints from ODP Leg 204. Earth Planet. Sci. Lett. **222**: 845–862. doi:10.1016/j.epsl.2004.03.035

Trembath-Reichert, E., D. A. Butterfield, and J. A. Huber. 2019. Active subseafloor microbial communities from Mariana back-arc venting fluids share metabolic strategies across different thermal niches and taxa. ISME J. **13**: 2264–2279. doi:10.1038/s41396-019-0431-y

Turner, P. J., and others. 2020. Methane seeps on the US Atlantic margin and their potential importance to populations of the commercially valuable Deep-Sea red crab, *Chaceon quinquedens*. Front. Mar. Sci. **7**: 75. doi:10.3389/fmars.2020.00075

Vigneron, A., and others. 2017. Comparative metagenomics of hydrocarbon and methane seeps of the Gulf of Mexico. Sci. Rep. **7**: 16015. doi:10.1038/s41598-017-16375-5

Watson, S. J., and others. 2020. Focused fluid seepage related to variations in accretionary wedge structure, Hikurangi margin, New Zealand. Geology **48**: 56–61. doi:10.1130/G46666.1

Acknowledgments

We would like to thank the captain, crew, scientists, and science communicators aboard NA072 and NA095 for their support of the work presented here. Funding to support this work came from NOAA Ocean Exploration Grant NA19OAR0110301 and NSF 2046800 and 1933165. MET acknowledges a fellowship from the Hanse-Wissenschaftskolleg (HWK), Delmenhorst, Germany. This is PMEL contribution number 5438. Open access publishing facilitated by National Institute of Water and Atmospheric Research, as part of the Wiley - National Institute of Water and Atmospheric Research agreement via the Council of Australian University Librarians.

Conflict of interest

The authors declare no conflicts of interest.

Submitted 20 December 2022
Revised 17 March 2024
Accepted 23 March 2024

Associate editor: Laura Bristow